α-decay chains of superheavy $^{265-279}$Mt isotopes

K. P. Santhosh* and C. Nithya

School of Pure and Applied Physics, Swami Anandatheertha Campus, Kannur University, Payyanur 670327, Kerala, India

(Received 8 September 2017; published 18 October 2017)

The α-decay chains of the isotopes $^{265-279}$Mt are predicted by comparing the α half-lives calculated within the Coulomb and proximity potential model for deformed nuclei of Santhosh *et al.* [Nucl. Phys. A **850**, 34 (2011)] with the spontaneous fission half-lives using the shell-effect-dependent formula of Santhosh and Nithya [Phys. Rev. C **94**, 054621 (2016)]. α half-lives also are calculated using different theoretical formalisms for comparison. The predicted half-lives and decay modes match well with the experimental results. The use of four different mass tables for calculating the α- decay energies indicates that the mass table of Wang *et al.* [Chin. Phys. C **41**, 030003 (2017)], which is based on the AME2016 atomic mass evaluation, is in better agreement with experimental results. The paper predicts long α chains from $^{265,267-269,271-273}$Mt with half-lives within experimental limits. The isotopes $^{274-276,278}$Mt exhibit 2α chains followed by spontaneous fission. The 2α chain of ^{266}Mt and the 4α chain of ^{270}Mt end with electron capture. The isotopes ^{277,279}Mt decay via spontaneous fission. We hope that the paper will open up new areas in this field.

DOI: 10.1103/PhysRevC.96.044613

I. INTRODUCTION

The studies on superheavy nuclei (SHN) have received much attention, both theoretically and experimentally, for the past few decades. The discussion about the limits of nuclear stability became important after the prediction of the magic island or the island of stability [1–5]. Two different experimental approaches, namely, the cold fusion reaction [6] and the hot fusion reaction [7] are used for the synthesis of SHN. Elements up to Nh ($Z = 113$) have been produced using cold fusion reaction at GSI, Darmstadt and Rikagaku Kenkyusho, Japan [8–10]. Hot fusion reactions are performed mainly at the Joint Institute for Nuclear Research-Flerov Laboratory of Nuclear Reactions, Dubna which produced elements up to Og ($Z = 118$) [11].

The detection of a SHN is possible only if its lifetime is longer than 1 μs. So the studies on the half-lives have considerable importance in predicting new SHN. Knowledge about the decay modes of nuclei in a very wide range of neutron and proton numbers is necessary for such predictions. The main decay modes of heavy nuclei and SHN are the α decay and spontaneous fission (SF). The α decay and SF are considered as the limiting factor that determines the stability of the heaviest nuclei. The newly synthesized SHN are identified with their α-decay chain which usually ends with SF.

The α-decay studies are performed using various theoretical approaches, such as the fission model [12], the cluster model [13], and the generalized liquid drop model [14]. Geiger-Nuttal-type formulas [15–17] and semiempirical relations [18] also are used for calculating the α-decay half-lives. One of the most uncertain quantities in SHN is their SF half-lives. The process of SF is more complicated as compared to the other decay modes. Many theoretical studies including the phenomenological ones [19–21] and dynamical approaches [22–24] are used for the prediction of SF half-lives.

In the present paper we have studied the α-decay chains of the isotopes of the element meitnerium (Mt) ($Z = 109$) within the Coulomb and proximity potential model for deformed nuclei (CPPMDN) [25]. The CPPMDN proposed by Santhosh *et al.* [25], has proved to be very successful in predicting the half-lives of SHN [26–29]. The element Mt (^{266}Mt) was identified first with the cold fusion reaction by Münzenberg *et al.* [30] by irradiating ^{209}Bi target with ^{58}Fe projectiles. The isotope ^{268}Mt was identified by Hofmann *et al.* [31] in the decay chain of the isotope ^{272}Rg, and the isotope ^{270}Mt was identified by Morita *et al.* [32] in the decay chain of ^{278}Nh. Oganessian *et al.* [33] has reported $^{274-278}$Mt in the decay chains of ^{282}Nh, ^{287,288}Mc, and ^{293,294}Ts.

The paper is organized as follows. In Sec. II a brief description of the CPPMDN [25] and the shell-effect-dependent formula of Santhosh and Nithya [34] are given. Section III contains the results and discussion, and Sec. IV represents the conclusions derived from the paper.

II. MODELS

A. The CPPMDN

The half-life of nuclei which decay through α emission can be calculated by means of the WKB approximation. The α-decay half-lives can be obtained using

$$T_{1/2} = \left(\frac{\ln 2}{\lambda}\right) = \left(\frac{\ln 2}{\nu P}\right), \tag{1}$$

where λ is the decay constant, ν is the assault frequency, and P is the barrier penetrability. The assault frequency ν can be calculated as

$$\nu = \left(\frac{\omega}{2\pi}\right) = \left(\frac{2E_v}{h}\right). \tag{2}$$

*drkpsanthosh@gmail.com

Here E_v is the empirical vibration energy, which is given by [35]

$$E_v = Q\left\{0.056 + 0.039 \exp\left[\frac{(4 - A_2)}{2.5}\right]\right\} \quad \text{for} \quad A_2 \geqslant 4. \tag{3}$$

The barrier penetrability P using the one-dimensional Wentzel-Kramers-Brillouin approximation is as follows:

$$P = \exp\left\{-\frac{2}{\hbar}\int_a^b \sqrt{2\mu(V-Q)}dz\right\}. \tag{4}$$

Here the mass parameter is replaced by $\mu = mA_1A_2/A$, where m is the nucleon mass and A_1, A_2 are the mass numbers of the daughter and the emitted cluster, respectively. V represents the interacting potential between two nuclei. The turning points a and b are determined from the equation $V(a) = V(b) = Q$, where Q is the energy released.

In the CPPMDN the interacting potential between two nuclei is taken as the sum of the deformed Coulomb potential, the deformed two-term proximity potential, and the centrifugal potential for both the touching configuration and the separated fragments. It is given by

$$V = V_C(r,\theta) + V_{P2}(r,\theta) + \frac{\hbar^2\ell(\ell+1)}{2\mu r^2}, \tag{5}$$

where $V_C(r,\theta)$ is the Coulomb interaction between the two deformed and oriented nuclei, $V_{P2}(r,\theta)$ is the two-term proximity potential, ℓ represents the angular momentum, and μ represents the reduced mass.

The Coulomb interaction between the two deformed and oriented nuclei [36] $V_C(r,\theta)$, with higher multipole deformations [37,38] is given as

$$V_C(r,\theta) = \frac{Z_1Z_2e^2}{r} + 3Z_1Z_2e^2 \sum_{\lambda,i=1,2} \frac{1}{2\lambda+1}\frac{R_{0i}^{\lambda}}{r^{\lambda+1}} Y_{\lambda}^{(0)}(\alpha_i) \times \left[\beta_{\lambda i} + \frac{4}{7}\beta_{\lambda i}^2 Y_{\lambda}^{(0)}(\alpha_i)\delta_{\lambda,2}\right]. \tag{6}$$

Here Z_1 and Z_2 are the atomic numbers of the daughter and the emitted cluster, r is the distance between fragment centers, and

$$R_i(\alpha_i) = R_{0i}\left[1 + \sum_{\lambda}\beta_{\lambda i}Y_{\lambda}^{(0)}(\alpha_i)\right], \tag{7}$$

where $R_{0i} = 1.28A_i^{1/3} - 0.76 + 0.8A_i^{-1/3}$. Here α_i is the angle between the radius vector and the symmetry axis of the ith nuclei (see Fig. 1 of Ref. [37]). The quadrupole interaction term proportional to $\beta_{21}\beta_{22}$ is neglected because of its short-range character.

The two-term proximity potential for the interaction between a deformed nucleus and a spherical nucleus given by Baltz and Bayman [39] is as follows:

$$V_{P2}(r,\theta) = 2\pi\left[\frac{R_1(\alpha)R_C}{R_1(\alpha)+R_C+S}\right]^{1/2}\left[\frac{R_2(\alpha)R_C}{R_2(\alpha)+R_C+S}\right]^{1/2} \times \left\langle\left[\varepsilon_0(S) + \frac{R_1(\alpha)+R_C}{2R_1(\alpha)R_C}\varepsilon_1(S)\right] \times \left[\varepsilon_0(S) + \frac{R_2(\alpha)+R_C}{2R_2(\alpha)R_C}\varepsilon_1(S)\right]\right\rangle^{1/2}, \tag{8}$$

where θ is the angle between the symmetry axis of the deformed nuclei and the line joining the centers of the two interacting nuclei, and α corresponds to the angle between the radius vector and the symmetry axis of the nuclei (see Fig. 5 of Ref. [39]). $R_1(\alpha)$ and $R_2(\alpha)$ are the principal radii of curvature of the daughter nuclei, R_C is the radius of the spherical cluster, S is the distance between the surfaces along the straight line connecting the fragments, and $\varepsilon_0(S)$ and $\varepsilon_1(S)$ are the one-dimensional slab-on-slab functions.

For the prescission (overlap) region, simple power-law interpolation [40] has been used. The potential for the internal part of the barrier is given as

$$V = a_0(L - L_0)^n \quad \text{for} \quad z < 0, \tag{9}$$

here $L = z + 2C_1 + 2C_2$ fm and $L_0 = 2C$ fm, where C, C_1, and C_2 are the Süsmann central radii of the parent nuclei, the daughter nuclei, and the emitted cluster, respectively. The constants a_0 and n are determined by the smooth matching of the two potentials at the touching point.

In the case of spherical nuclei, (in the CPPM), the interacting barrier is given by

$$V = \frac{Z_1Z_2e^2}{r} + V_P(z) + \frac{\hbar^2\ell(\ell+1)}{2\mu r^2} \quad \text{for} \quad z > 0, \tag{10}$$

where z is the distance between the near surfaces of the fragments. $V_P(z)$ is the proximity potential given by Blocki *et al.* [41] and Blocki and Świątecki [42] as

$$V_P(z) = 4\pi\gamma b\left[\frac{C_1C_2}{(C_1+C_2)}\right]\Phi\left(\frac{z}{b}\right), \tag{11}$$

with the nuclear surface tension coefficient,

$$\gamma = 0.9517[1 - 1.7826(N-Z)^2/A^2]\,\text{MeV/fm}^2. \tag{12}$$

Here N, Z, and A represent the neutron, the proton, and the mass number of the parent nuclei. Φ represents the universal proximity potential [42] given as

$$\Phi(\varepsilon) = -4.41e^{-\varepsilon/0.7176} \quad \text{for} \quad \varepsilon > 1.9475, \tag{13}$$

$$\Phi(\varepsilon) = -1.7817 + 0.9270\varepsilon + 0.0169\varepsilon^2 - 0.05148\varepsilon^3 \quad \text{for} \quad 0 \leqslant \varepsilon \leqslant 1.9475, \tag{14}$$

with $\varepsilon = z/b$, where $b \approx 1$fm is the width (diffuseness) of the nuclear surface. The Süsmann central radii C_i of the fragments are related to the sharp radii R_i as

$$C_i = R_i - \left(\frac{b^2}{R_i}\right)\text{fm}. \tag{15}$$

For R_i, we use a semiempirical formula in terms of mass number A_i as [41]

$$R_i = 1.28A_i^{1/3} - 0.76 + 0.8A_i^{-1/3}\text{fm}. \tag{16}$$

B. Shell-effect-dependent formula for spontaneous fission half-lives

Spontaneous fission was described early within the geometrical framework of the charged liquid drop model [43]. The first semiempirical formula for calculating the spontaneous fission half-lives was proposed by Swiatecki [19]. Theoretically the quantum tunneling effect is considered as the underlying mechanism of SF. The probability of tunneling through a potential barrier depends exponentially on the square root of the barrier height and inversely related to the fissionability parameter. The fissionability parameter $\frac{Z^2}{A}$ and the isospin effect $\frac{N-Z}{N+Z}$ play an important role in determining the SF half-lives of heavy and superheavy nuclei. Considering these two factors our group had developed a semiempirical formula for calculating the SF half-lives [44]. Since the shell structure also plays an important role in determining SF half-lives, by including the shell correction term, we modified the previous formula, and it is given by [34]

$$\log_{10}(T_{1/2}/\mathrm{yr}) = a\frac{Z^2}{A} + b\left(\frac{Z^2}{A}\right)^2 + c\left(\frac{N-Z}{N+Z}\right) + d\left(\frac{N-Z}{N+Z}\right)^2 + eE_{\mathrm{shell}} + f, \quad (17)$$

where $a = -43.25203$, $b = 0.49192$, $c = 3674.3927$, $d = -9360.6$, $e = 0.8930$, and $f = 578.56058$. E_{shell} is the shell correction energy taken from Ref. [45]. The estimated standard deviation from the experimental SF half-life values of 45 nuclei is found to be 1.6972, i.e., the average deviation between the theoretical and the experimental spontaneous fission half-lives is less than 10^2 times. This level of agreement is very satisfactory since SF is a much more complex process than α decay.

III. RESULTS AND DISCUSSION

In the present paper we have studied the α-decay chains of the isotopes $^{265-279}$Mt. The α-decay chains are predicted by comparing the α half-lives of each isotope with the corresponding spontaneous fission half-lives. Those isotopes with α half-lives less than SF half-lives will survive fission and hence decay through α emission. The α half-lives are calculated using the CPPMDN. The CPPM [46], the Viola-Seaborg-Sobiczewski semiempirical relation [18,47], the universal curve (UNIV) of Poenaru *et al.* [48,49], the analytical formula of Royer [50], and the universal decay law (UDL) of Qi and co-workers [15,16] have also been used for a theoretical comparison. The detailed description of all these theoretical formalisms can be seen in Ref. [26]. The SF half-lives are calculated using the shell-effect-dependent formula of Santhosh and Nithya [34] and the semiempirical formula of Xu *et al.* [51].

It should be noted that the empirical relationships for α-decay half-lives obtained in Refs. [15,47–50] have not taken into account any angular momentum and/or parity corrections. In the case of even-even nuclei, the spin and parity values of the parent and daughter nuclei usually are ignored. But in the case of even-odd, odd-even, and odd-odd nuclei, the transitions may occur with different spins and parities of the parent and daughter nuclei. Consequently the α particle may take away a nonzero angular momentum ℓ. So the effect of the orbital angular momentum the emitted α particle should be taken into account while studying α decay. Denisov *et al.* [52] performed the improved parametrization of the unified model for α decay and α capture (UMADAC) with the inclusion of the orbital momentum term. The parameter values of the UMADAC have been obtained by using the updated values of the α decay half-lives, the binding energies of the nuclei, the spins of the parent and daughter nuclei, and the surface deformation parameters of the daughter nuclei. The available α-decay values are well described by this empirical relationship for α-decay half-lives which takes into account the spin-parity properties of the parent and daughter nuclei. Empirical expressions depending on the angular momentum of the α particle for the even-odd, odd-even, and odd-odd nuclei are proposed by Royer [53] in order to find the α half-lives. The introduction of new terms simulating the centrifugal effects and the hindrance of α emission with odd values of ℓ improved the efficiency of the formulas even though the terms are semiempirical. Recently Zhang *et al.* [54] improved the formula of Sahu *et al.* [55] by introducing a precise radius formula and an analytic expression for preformation probability and calculated the α-decay half-lives of 421 nuclei. The formula of Sahu *et al.* [55] is similar to the UDL [15,16] but with an inbuilt angular momentum dependence. It was shown that the accuracy of semiempirical relationship proposed by Zhang *et al.* [54] was improved significantly as compared to the formula of Sahu *et al.* [55].

For calculating the α half-lives, calculation of α-decay energies, that is, the Q value plays an important role. Q values are obtained by the atomic mass difference between the ground states of the parent and decay fragments. For calculating the Q values, we have used the recent mass table of Wang *et al.* [56], which is based on the AME2016 atomic mass evaluation. The screening of atomic electrons [57,58] also is taken into consideration while calculating the Q values using the mass table of Wang *et al.* [56]. Since the α-decay energies are very sensitive to the mass excess values, the half-lives of the experimentally synthesized isotopes of Mt also are calculated using the Weizsäcker-Skyrme 4 + radial basis function (WS4 + RBF) model [59], the mass table of Möller *et al.* [45], and the mass table of Koura *et al.* [60].

Tables I–V show the Q values, the decay half-lives, and the decay modes for all the experimentally synthesized isotopes of Mt. The first column represents the parent nuclei in the α-decay chains. The second column represents the Q values calculated using different mass models and the experimental Q values [30–33]. One can see from the tables that the Q values calculated using different models are different from each other. For example, in the case of ^{266}Mt, the experimental Q value reported by Münzenberg *et al.* [30] is 11.100 MeV. Using the mass table of Wang *et al.* [56] the Q value obtained for ^{266}Mt is 11.048 MeV, whereas, in the WS4 mass table [59], the mass table of Möller *et al.* [45] and the mass table of Koura *et al.* [60] give the Q values as 11.311, 10.755, and 11.118 MeV, respectively. It is well known that the α-decay half-lives are extremely sensitive to the Q values. A change in the Q value by 1 MeV will make several order changes in the calculation

TABLE I. The comparison of the calculated α-decay half-lives with the spontaneous fission half-lives for the isotopes ^{266,268}Mt and their decay products. The experimental half-lives and the decay modes of the isotopes are taken from Refs. [30,31].

Parent	Q_α (MeV)	T_{SF} (s)		$T^{\alpha}_{1/2}$ (s)						Expt.	Mode of decay	
Nuclei		Xu *et al.* [51]	KPS	CPPMDN	CPPM	VSS	UNIV	Royer [50]	UDL	half-lives (s)	Th.	Expt.
^{266}Mt	11.048[a]	1.490×10^{-4}	2.800×10^{-3}	1.916×10^{-6}	1.914×10^{-4}	2.786×10^{-4}	3.018×10^{-5}	9.922×10^{-5}	3.277×10^{-5}	5.000×10^{-3}	α	α
	11.311[b]			1.212×10^{-6}	8.599×10^{-5}	3.036×10^{-4}	5.133×10^{-5}	1.131×10^{-4}	1.498×10^{-5}			
	10.755[c]			2.910×10^{-5}	2.173×10^{-3}	6.208×10^{-3}	9.761×10^{-4}	2.870×10^{-3}	3.689×10^{-4}			
	11.118[d]			3.476×10^{-6}	2.511×10^{-4}	8.434×10^{-4}	1.387×10^{-4}	3.380×10^{-4}	4.433×10^{-5}			
	11.100[e]			9.897×10^{-7}	2.885×10^{-4}	9.305×10^{-4}	1.527×10^{-4}	3.755×10^{-4}	4.920×10^{-5}			
^{262}Bh	10.367[a]	1.059×10^{-3}	1.103×10^{-2}	7.283×10^{-6}	1.763×10^{-3}	2.235×10^{-3}	2.335×10^{-4}	7.976×10^{-4}	2.872×10^{-4}	2.230×10^{-2}	α	α
	10.311[b]			2.977×10^{-5}	7.418×10^{-3}	1.929×10^{-2}	3.213×10^{-3}	8.898×10^{-3}	1.182×10^{-3}			
	10.105[c]			1.064×10^{-4}	2.709×10^{-2}	6.584×10^{-2}	1.079×10^{-2}	3.321×10^{-2}	4.354×10^{-3}			
	10.457[d]			1.169×10^{-5}	2.854×10^{-3}	8.225×10^{-3}	1.388×10^{-3}	3.567×10^{-3}	4.780×10^{-4}			
^{258}Db	9.555[a]	7.043×10^{-1}	1.538	1.182	1.987	1.512	1.394×10^{-1}	5.647×10^{-1}	2.829×10^{-1}	1.290[f]	α	EC
	9.499[b]			1.955×10^{-1}	3.306×10^{-1}	6.574×10^{-1}	1.163×10^{-1}	3.648×10^{-1}	4.867×10^{-2}			
	9.515[c]			1.103×10^{-1}	1.872×10^{-1}	5.914×10^{-1}	1.046×10^{-1}	3.256×10^{-1}	4.350×10^{-2}			
	9.755[d]			1.566×10^{-4}	5.433×10^{-2}	1.274×10^{-1}	2.274×10^{-2}	6.264×10^{-2}	8.512×10^{-3}			
^{268}Mt	10.718[a]	1.793×10^{-2}	2.796	5.755×10^{-5}	2.602×10^{-3}	7.641×10^{-3}	3.011×10^{-4}	3.294×10^{-3}	4.265×10^{-4}	4.230×10^{-3}	α	α
	10.872[b]			2.290×10^{-5}	1.024×10^{-3}	3.233×10^{-3}	4.773×10^{-4}	1.311×10^{-3}	1.711×10^{-4}			
	10.025[c]			4.728×10^{-3}	2.236×10^{-1}	4.738×10^{-1}	6.481×10^{-2}	2.746×10^{-1}	3.411×10^{-2}			
	10.768[d]			4.258×10^{-5}	1.918×10^{-3}	5.763×10^{-3}	8.404×10^{-4}	2.435×10^{-3}	3.161×10^{-4}			
	10.294[e]			8.100×10^{-4}	3.767×10^{-2}	9.096×10^{-2}	1.267×10^{-2}	4.683×10^{-2}	5.914×10^{-3}			
^{264}Bh	10.017[a]	9.823×10^{-2}	2.802	3.989×10^{-4}	4.630×10^{-2}	1.129×10^{-1}	4.281×10^{-3}	5.438×10^{-2}	7.157×10^{-3}	9.440×10^{-1}	α	α
	9.929[b]			7.128×10^{-4}	8.337×10^{-02}	1.945×10^{-1}	2.917×10^{-2}	9.747×10^{-2}	1.275×10^{-2}			
	9.605[c]			6.476×10^{-3}	7.773×10^{-1}	1.538	2.276×10^{-01}	8.960×10^{-1}	1.147×10^{-1}			
	10.137[d]			1.830×10^{-4}	2.102×10^{-2}	5.433×10^{-2}	8.260×10^{-3}	2.482×10^{-2}	3.292×10^{-3}			
	9.365[e]			3.576×10^{-2}	4.368	7.634	1.125	4.996	6.290×10^{-1}			
^{260}Db	9.545[a]	4.146	2.301×10^{1}	6.046×10^{-4}	2.211×10^{-1}	4.858×10^{-1}	1.895×10^{-2}	2.421×10^{-1}	3.273×10^{-2}	3.640×10^{-1}	α	α
	9.601[b]			1.485×10^{-1}	1.497×10^{-1}	3.396×10^{-1}	5.570×10^{-2}	1.648×10^{-1}	2.237×10^{-2}			
	9.335[c]			2.458×10^{-3}	9.848×10^{-1}	1.941	3.165×10^{-1}	1.071	1.426×10^{-1}			
	9.605[d]			1.444×10^{-1}	1.456×10^{-1}	3.299×10^{-1}	5.412×10^{-2}	1.598×10^{-1}	2.170×10^{-2}			
	9.156[e]			9.553×10^{-3}	3.660	6.558	1.069	3.958	5.201×10^{-1}			
^{256}Lr	8.864[a]	1.008×10^{3}	1.985×10^{3}	2.149	5.761	1.003×10^{1}	3.980×10^{-1}	5.879	8.005×10^{-1}	5.580×10^{1}	α	α
	8.742[b]			5.534	1.481×10^{1}	2.401×10^{1}	4.396	1.502×10^{1}	2.024			
	8.815[c]			3.135	8.397	1.421×10^{1}	2.594	8.544	1.159			
	8.904[d]			1.582	4.245	7.562	1.377	4.338	5.926×10^{-1}			
	8.465[e]			5.107×10^{1}	1.359×10^{2}	1.878×10^{2}	3.496×10^{1}	1.370×10^{2}	1.803×10^{1}			

[a] Q value calculated using the mass excess taken from the mass table of Wang *et al.* [56].
[b] Q value calculated using the mass excess taken from the WS4+RBF mass model [59].
[c] Q value calculated using the mass excess taken from the mass table of Möller *et al.* [45].
[d] Q value calculated using the mass excess taken from the mass table of Koura *et al.* [60].
[e] Experimental Q value taken from Refs. [30,31].
[f] Experimental electron capture half-life taken from Ref. [30].

TABLE II. The comparison of the calculated α-decay half-lives with the spontaneous fission half-lives for the isotopes ^{270}Mt and their decay products. The experimental half-lives and the decay modes of the isotopes are taken from Ref. [32].

Parent	Q_α(MeV)	T_{SF} (s)		$T^{\alpha}_{1/2}$ (s)						Expt.	Mode of decay	
nuclei		Xu *et al.* [51]	KPS	CPPMDN	CPPM	VSS	UNIV	Royer [50]	UDL	half-lives (s)	Th.	Expt.
^{270}Mt	10.238[a]	4.686×10^{-2}	4.683×10^{1}	1.496×10^{-3}	5.018×10^{-2}	1.273×10^{-1}	4.195×10^{-3}	6.173×10^{-2}	7.843×10^{-3}	4.44×10^{-1}	α	α
	10.090[b]			3.944×10^{-3}	1.335×10^{-1}	3.156×10^{-1}	4.011×10^{-2}	1.633×10^{-1}	2.056×10^{-2}			
	9.565[c]			1.472×10^{-1}	5.137	9.357	1.164	6.172	7.513×10^{-1}			
	10.488[d]			3.046×10^{-4}	1.006×10^{-2}	2.872×10^{-2}	3.768×10^{-3}	1.251×10^{-2}	1.613×10^{-3}			
	10.260[e]			1.297×10^{-3}	4.346×10^{-2}	1.117×10^{-1}	1.436×10^{-2}	5.363×10^{-2}	6.822×10^{-3}			
^{266}Bh	9.477[a]	1.811×10^{-1}	3.115×10^{1}	2.444×10^{-2}	1.791	3.593	1.147×10^{-1}	2.045	2.621×10^{-1}	5.26	α	α
	9.498[b]			2.105×10^{-2}	1.540	3.125	4.266×10^{-1}	1.761	2.260×10^{-1}			
	8.855[c]			2.606	1.983×10^{2}	2.839×10^{2}	3.906×10^{1}	2.221×10^{2}	2.718×10^{1}			
	9.897[d]			1.345×10^{-3}	9.570×10^{-2}	2.376×10^{-1}	3.293×10^{-2}	1.111×10^{-1}	1.464×10^{-2}			
	9.390[e]			4.567×10^{-2}	3.365	6.443	8.781×10^{-1}	3.827	4.874×10^{-1}			
^{262}Db	9.095[a]	6.941	8.887×10^{1}	2.833×10^{-2}	5.345	9.985	3.363×10^{-1}	5.711	7.543×10^{-1}	1.26×10^{2}	α	α
	9.044[b]			4.144×10^{-2}	7.853	1.428×10^{1}	2.153	8.383	1.103			
	8.845[c]			1.888×10^{-1}	3.634×10^{1}	5.922×10^{1}	8.983	3.862×10^{1}	5.002			
	9.415[d]			2.797×10^{-3}	5.132×10^{-1}	1.138	1.717×10^{-1}	5.546×10^{-1}	7.501×10^{-2}			
	8.630[e]			1.030	2.016×10^{2}	2.908×10^{2}	4.459×10^{1}	2.132×10^{2}	2.714×10^{1}			
^{258}Lr	8.954[a]	1.603×10^{3}	4.485×10^{3}	1.613	2.693	5.324	1.974×10^{-1}	2.733	3.785×10^{-1}	3.78	α	α
	8.812[b]			4.785	7.963	1.447×10^{1}	2.442	8.005	1.096			
	8.645[c]			1.778×10^{1}	2.946×10^{1}	4.881×10^{1}	8.294	2.956×10^{1}	3.992			
	8.794[d]			5.503	9.152	1.654×10^{1}	2.792	9.239	1.263			
	8.660[e]			1.578×10^{1}	2.615×10^{1}	4.373×10^{1}	7.427	2.627×10^{1}	3.553			
^{254}Md	7.842[a]	1.771×10^{6}	2.585×10^{6}	9.663×10^{2}	4.063×10^{3}	4.656×10^{3}	1.764×10^{2}	3.788×10^{3}	5.034×10^{2}	6.00×10^{2}[f]	α	EC
	7.875[b]			7.183×10^{2}	3.021×10^{3}	3.555×10^{3}	7.250×10^{2}	2.833×10^{3}	3.778×10^{2}			
	7.865[c]			9.233	3.304×10^{3}	3.855×10^{3}	7.873×10^{2}	3.092×10^{3}	4.119×10^{2}			
	8.002[d]			2.333×10^{2}	9.832×10^{2}	1.248×10^{3}	2.503×10^{2}	9.192×10^{2}	1.241×10^{2}			

[a] Q value calculated using the mass excess taken from the mass table of Wang *et al.* [56].
[b] Q value calculated using the mass excess taken from the WS4+RBF mass model [59].
[c] Q value calculated using the mass excess taken from the mass table of Möller *et al.* [45].
[d] Q value calculated using the mass excess taken from the mass table of Koura *et al.* [60]
[e] Experimental Q value taken from Ref. [32].
[f] Experimental electron capture half-life taken from Ref. [32].

TABLE III. The comparison of the calculated α-decay half-lives with the spontaneous fission half-lives for the isotopes ^{274,275}Mt and their decay products. The experimental half-lives and the decay modes of the isotopes are taken from Ref. [33].

Parent	Q_α(MeV)	T_{SF} (s)		$T_{1/2}^{\alpha}$ (s)						Expt.	Mode of decay	
nuclei		Xu *et al.* [51]	KPS	CPPMDN	CPPM	VSS	UNIV	Royer [50]	UDL	half-lives (s)	Th.	Expt.
^{274}Mt	10.648[a]	2.791×10^{-2}	1.257×10^{1}	3.618×10^{-4}	3.184×10^{-3}	1.138×10^{-2}	3.516×10^{-4}	3.927×10^{-3}	5.203×10^{-4}	4.400×10^{-1}	α	α
	10.284[b]			3.573×10^{-3}	3.197×10^{-2}	9.642×10^{-2}	2.753×10^{-3}	3.878×10^{-2}	5.031×10^{-3}			
	10.005[c]			2.246×10^{-2}	2.034×10^{-1}	5.372×10^{-1}	5.826×10^{-2}	2.443×10^{-1}	3.117×10^{-2}			
	10.028[d]			1.924×10^{-2}	1.741×10^{-1}	4.644×10^{-1}	5.044×10^{-2}	2.090×10^{-1}	2.670×10^{-2}			
	10.200[e]			2.717×10^{-4}	6.165×10^{-3}	1.608×10^{-1}	1.767×10^{-2}	6.706×10^{-2}	8.657×10^{-3}			
^{270}Bh	9.117[a]	3.543×10^{-2}	5.394×10^{1}	7.135×10^{-1}	2.218×10^{1}	4.272×10^{1}	1.109	2.463×10^{1}	3.135	6.100×10^{1}	α	α
	8.887[b]			4.223	1.323×10^{2}	2.247×10^{2}	5.670	1.461×10^{2}	1.828×10^{1}			
	8.325[c]			5.097×10^{1}	1.406×10^{4}	1.723×10^{4}	2.106×10^{3}	1.535×10^{4}	1.837×10^{3}			
	9.387[d]			9.620×10^{-2}	2.960	6.583	7.683×10^{-1}	3.312	4.299×10^{-1}			
	9.060[e]			1.102	3.431×10^{1}	6.400×10^{1}	7.480	3.799×10^{1}	4.816			
^{266}Db	8.265[a]	7.694×10^{-1}	1.243×10^{2}	4.858×10^{2}	3.694×10^{3}	4.970×10^{3}	1.315×10^{2}	3.798×10^{3}	4.781×10^{2}	1.320×10^{3}	SF	SF
	7.918[b]			1.481×10^{3}	8.175×10^{4}	8.904×10^{4}	2.317×10^{3}	8.415×10^{4}	1.027×10^{4}			
	7.445[c]			2.797×10^{4}	7.819×10^{6}	6.215×10^{6}	9.576×10^{5}	8.031×10^{6}	9.358×10^{5}			
	8.805[d]			8.175×10^{-1}	4.288×10^{1}	7.911×10^{1}	1.028×10^{1}	4.455×10^{1}	5.866			
^{275}Mt	10.538[a]	9.492×10^{-3}	1.177	7.311×10^{-4}	6.089×10^{-3}	9.762×10^{-3}	6.228×10^{-4}	2.302×10^{-3}	9.832×10^{-4}	2.000×10^{-2}	α	α
	10.209[b]			5.950×10^{-3}	5.031×10^{-2}	6.915×10^{-2}	4.114×10^{-3}	1.648×10^{-2}	7.860×10^{-3}			
	10.105[c]			1.179×10^{-2}	1.001×10^{-1}	1.310×10^{-1}	3.027×10^{-2}	3.134×10^{-2}	1.550×10^{-2}			
	9.918[d]			4.140×10^{-2}	3.546×10^{-1}	4.230×10^{-1}	9.658×10^{-2}	1.018×10^{-1}	5.378×10^{-2}			
	10.480[e]			1.051×10^{-3}	8.774×10^{-3}	1.372×10^{-2}	3.269×10^{-3}	3.241×10^{-3}	1.411×10^{-3}			
^{271}Bh	9.477[a]	7.582×10^{-3}	7.801	7.528×10^{-2}	1.487	1.635	9.458×10^{-2}	3.944×10^{-1}	2.177×10^{-1}	1.500	α	α
	9.160[b]			7.711×10^{-1}	1.543×10^{1}	1.437×10^{1}	7.934×10^{-1}	3.515	2.192			
	8.715[c]			1.856	5.074×10^{2}	3.684×10^{2}	9.226×10^{1}	9.195×10^{1}	6.880×10^{1}			
	9.217[d]			5.030×10^{-1}	1.004×10^{1}	9.631	2.375	2.350	1.433			
	9.420[e]			1.134×10^{-1}	2.245	2.393	5.910×10^{-1}	5.789×10^{-1}	3.265×10^{-1}			
^{267}Db	7.965[a]	8.159×10^{-2}	4.806×10^{1}	9.557×10^{2}	5.123×10^{4}	2.700×10^{4}	1.487×10^{3}	7.012×10^{3}	6.432×10^{3}	4.680×10^{3}	SF	SF
	7.743[b]			7.506×10^{3}	4.061×10^{5}	1.859×10^{5}	1.018×10^{4}	4.894×10^{4}	4.998×10^{4}			
	7.275[c]			7.841×10^{5}	4.319×10^{7}	1.439×10^{7}	4.874×10^{6}	3.909×10^{6}	5.085×10^{6}			
	8.665[d]			6.081×10^{1}	1.262×10^{2}	1.014×10^{2}	2.804×10^{1}	2.531×10^{1}	1.701×10^{1}			

[a] Q value calculated using the mass excess taken from the mass table of Wang *et al.* [56].
[b] Q value calculated using the mass excess taken from the WS4+RBF mass model [59].
[c] Q value calculated using the mass excess taken from the mass table of Möller *et al.* [45].
[d] Q value calculated using the mass excess taken from the mass table of Koura *et al.* [60].
[e] Experimental Q value taken from Ref. [33].

TABLE IV. The comparison of the calculated α-decay half-lives with the spontaneous fission half-lives for the isotopes ^{276,277}Mt and their decay products. The experimental half-lives and the decay modes of the isotopes are taken from Ref. [33].

Parent	Q_α(MeV)	T_{SF} (s)		$T^{\alpha}_{1/2}$ (s)						Expt.	Mode of decay	
nuclei		Xu *et al.* [51]	KPS	CPPMDN	CPPM	VSS	UNIV	Royer [50]	UDL	half-lives (s)	Th.	Expt.
^{276}Mt	10.158[a]	4.952×10^{-3}	1.909×10^{-1}	8.505×10^{-3}	6.793×10^{-2}	2.075×10^{-1}	5.354×10^{-3}	8.115×10^{-2}	1.054×10^{-2}	4.500×10^{-1}	α	α
	9.930[b]			3.913×10^{-2}	3.150×10^{-1}	8.652×10^{-1}	2.137×10^{-2}	3.749×10^{-1}	4.803×10^{-2}			
	9.925[c]			4.048×10^{-2}	3.260×10^{-1}	8.904×10^{-1}	8.909×10^{-2}	3.866×10^{-1}	4.952×10^{-2}			
	9.788[d]			1.040×10^{-1}	8.408×10^{-1}	2.143	2.130×10^{-1}	9.910×10^{-1}	1.259×10^{-1}			
	10.030[e]			1.991×10^{-2}	1.597×10^{-1}	4.595×10^{-1}	4.626×10^{-2}	1.903×10^{-1}	2.453×10^{-2}			
^{272}Bh	9.357[a]	3.926×10^{-3}	1.067	1.731×10^{-1}	3.431	8.071	2.007×10^{-1}	3.794	4.959×10^{-1}	1.090×10^{1}	α	α
	9.182[b]			6.318×10^{-1}	1.261×10^{1}	2.701×10^{1}	6.548×10^{-1}	1.386×10^{1}	1.790			
	8.975[c]			2.304×10^{-1}	6.164×10^{1}	1.179×10^{2}	1.278×10^{1}	6.736×10^{1}	8.566			
	9.117[d]			1.032	2.063×10^{1}	4.272×10^{1}	4.617	2.267×10^{1}	2.913			
	9.180[e]			6.414×10^{-1}	1.280×10^{1}	2.738×10^{1}	2.957	1.406×10^{1}	1.815			
^{268}Db	8.305[a]	4.163×10^{-2}	1.363×10^{1}	4.610×10^{1}	2.436×10^{3}	3.607×10^{3}	8.848×10^{1}	2.477×10^{3}	3.160×10^{2}	9.360×10^{4}	SF	SF
	7.983[b]			1.564×10^{2}	4.195×10^{4}	5.090×10^{4}	1.227×10^{3}	4.248×10^{4}	5.268×10^{3}			
	7.315[c]			4.995×10^{5}	2.748×10^{7}	2.146×10^{7}	3.147×10^{6}	2.795×10^{7}	3.247×10^{6}			
	8.515[d]			2.729×10^{1}	4.149×10^{2}	6.960×10^{2}	8.500×10^{1}	4.234×10^{2}	5.499×10^{1}			
^{277}Mt	9.968[a]	4.127×10^{-4}	1.108×10^{-2}	3.823×10^{-2}	2.346×10^{-1}	3.081×10^{-1}	1.622×10^{-2}	6.800×10^{-2}	3.569×10^{-2}	5.000×10^{-3}	SF	SF
	9.682[b]			2.755×10^{-1}	1.712	1.952	9.765×10^{-2}	4.351×10^{-1}	2.536×10^{-1}			
	9.755[c]			1.651×10^{-1}	1.022	1.210	2.542×10^{-1}	2.691×10^{-1}	1.526×10^{-1}			
	9.648[d]			3.504×10^{-1}	2.180	2.443	5.110×10^{-1}	5.451×10^{-1}	3.217×10^{-1}			

[a] Q value calculated using the mass excess taken from the mass table of Wang *et al.* [56].
[b] Q value calculated using the mass excess taken from the WS4+RBF mass model [59].
[c] Q value calculated using the mass excess taken from the mass table of Möller *et al.* [45].
[d] Q value calculated using the mass excess taken from the mass table of Koura *et al.* [60].
[e] Experimental Q value taken from Ref. [33].

TABLE V. The comparison of the calculated α-decay half-lives with the spontaneous fission half-lives for the isotopes ^{278}Mt and their decay products. The experimental half-lives and the decay modes of the isotopes are taken from Ref. [33].

Parent	Q_α(MeV)	T_{SF} (s)		$T^{\alpha}_{1/2}$ (s)						Expt.	Mode of decay	
nuclei		Xu *et al.* [51]	KPS	CPPMDN	CPPM	VSS	UNIV	Royer [50]	UDL	half-lives (s)	Th.	Expt.
^{278}Mt	9.688[a]	2.081×10^{-4}	2.875×10^{-2}[f]	1.348×10^{-2}	1.583	4.122	9.040×10^{-2}	1.840	2.343×10^{-1}	4.500	α	α
	9.553[b]			1.523×10^{-2}	4.166	1.012×10^{1}	9.250×10^{-1}	4.818	6.082×10^{-1}			
	9.235[c]			3.672×10^{-1}	4.414×10^{1}	9.111×10^{1}	8.307	5.077×10^{1}	6.273			
	9.578[d]			2.843×10^{-2}	3.478	8.562	7.830×10^{-1}	4.027	5.092×10^{-1}			
	9.580[e]			4.847×10^{-1}	3.428	8.466	7.743×10^{-1}	3.979	5.031×10^{-1}			
^{274}Bh	8.997[a]	1.362×10^{-4}	4.535[f]	3.119×10^{-1}	4.841×10^{1}	1.008×10^{2}	2.208	5.240×10^{1}	6.738	4.400×10^{1}	α	α
	8.795[b]			3.639×10^{-1}	5.656×10^{1}	4.454×10^{2}	4.500×10^{1}	2.580×10^{2}	3.268×10^{1}			
	8.745[c]			2.260	3.574×10^{2}	6.455×10^{2}	6.537×10^{1}	3.842×10^{2}	4.847×10^{1}			
	8.937[d]			4.961×10^{-1}	7.733×10^{1}	1.558×10^{2}	1.565×10^{1}	8.360×10^{1}	1.070×10^{1}			
	8.940[e]			7.708	7.553×10^{1}	1.522×10^{2}	1.529×10^{1}	8.155×10^{1}	1.044×10^{1}			
^{270}Db	8.315[a]	8.452×10^{-4}	1.418×10^{1}[f]	9.338×10^{1}	2.085×10^{3}	3.331×10^{3}	7.563×10^{1}	2.093×10^{3}	2.699×10^{2}	5.400×10^{4}	SF	SF
	8.204[b]			6.106×10^{1}	1.361×10^{3}	8.186×10^{3}	9.512×10^{2}	5.497×10^{3}	7.020×10^{2}			
	7.915[c]			3.222×10^{3}	7.289×10^{4}	9.117×10^{4}	1.100×10^{4}	7.313×10^{4}	9.101×10^{3}			
	8.255[d]			1.563×10^{2}	3.495×10^{3}	5.387×10^{3}	6.225×10^{2}	3.508×10^{3}	4.500×10^{2}			

[a] Q value calculated using the mass excess taken from the mass table of Wang *et al.* [56].
[b] Q value calculated using the mass excess taken from the WS4+RBF mass model [59].
[c] Q value calculated using the mass excess taken from the mass table of Möller *et al.* [45].
[d] Q value calculated using the mass excess taken from the mass table of Koura *et al.* [60].
[e] Experimental Q value taken from Ref. [33].
[f] SF half-lives from Smolańczuck *et al.* [24].

of the half-lives. For example, in the case of ^{270}Bh, the Q value calculated using the mass table of Wang *et al.* [56] is 9.117 MeV, and the corresponding half-life using the CPPM is 2.218×10^1 s. But with the mass table of Möller *et al.* [45], the Q value for the same isotope is 8.325 MeV, and the half-life is 1.406×10^4 s. The sensitivity of the Q value to the mass model, makes the prediction of half-lives with good accuracy, very difficult. From the tables, it is seen that, for the decay chains of the isotopes of Mt, the Q values calculated using the mass table of Wang *et al.* [56] are in better agreement with the experimental Q values. The WS4 mass table [59] also gives a reasonable agreement. The deviation from the experimental Q value is larger while using the mass table of Koura *et al.* [60]. So it is clear that the α-decay energies obtained using the mass table of Wang *et al.* [56] are very satisfactorily in agreement with the experimental Q values of the different isotopes in the decay chain of Mt.

Recently Bao *et al.* [61] has performed theoretical predictions for the decay chain of the nuclei $^{293,295-297}$Og. In the study, to test the sensitivity of the α-decay half-lives with the changes in Q value, the authors have considered the mass model of Wang *et al.* [62], the WS4 mass model [59], and the two-center shell model (TCSM) [63]. It was found that the Q values obtained from the mass table of Wang *et al.* [62] are in good agreement with the experimental data. The decay properties of the isotope ^{296}Og were analyzed by Sobiczewski [64], and it is seen that the Q value varies between 10.43 and 13.33 MeV using nine different mass models. The study reveals a very careful choice of mass model to calculate realistic Q values. The best description of ^{296}Og is obtained by the TCSM [63] and the WS series models [59,65]. Similar studies have been performed by the same author in the case of ^{294}Og using five different mass models [66]. Illustrations of the accuracy of the nuclear mass models also were performed by Litvinov *et al.* [67], and the authors found that among the seven mass models tested, the best accuracy is obtained for the WS4 + RBF model [59]. Wang *et al.* [68] have studied the α-decay half-lives of SHN with $Z \geqslant 100$ using 20 mass models and 18 empirical formulas and found that the WS4 mass model [59] is the most accurate one to reproduce the experimental Q values.

In the present paper, the predictions on the half-lives for the isotopes $^{266,268,270,274-278}$Mt are given in columns 3–11 of Tables I–V. Columns 3 and 4 represent the SF half-lives calculated by the semiempirical formula of Xu *et al.* [51] and the shell-effect-dependent formula of Santhosh and Nithya [34]. The SF half-lives with the shell-effect-dependent formula is given as KPS in the tables. The semiempirical formula of Xu *et al.* [51] originally is made to fit the SF half-lives of even-even nuclei. Since we have considered only the odd-Z (i.e., odd-even and odd-odd) nuclei in the present paper, we have taken the average of the SF half-lives of the corresponding neighboring even-even nuclei. The $T_{\mathrm{sf}}^{\mathrm{av}}$'s of two neighboring even-even nuclei have been taken in the case of odd-even nuclei, and the $T_{\mathrm{sf}}^{\mathrm{av}}$'s of four neighboring even-even nuclei have been taken while dealing with odd-odd nuclei. Columns 5–10 represent the α half-lives using the CPPMDN [25], the CPPM [46], the VSS [18,47], the UNIV [48,49], the analytical formula of Royer [50], and the UDL [15,16]. The half-lives are calculated for different Q values obtained with different mass tables. In many cases order differences in half-life values

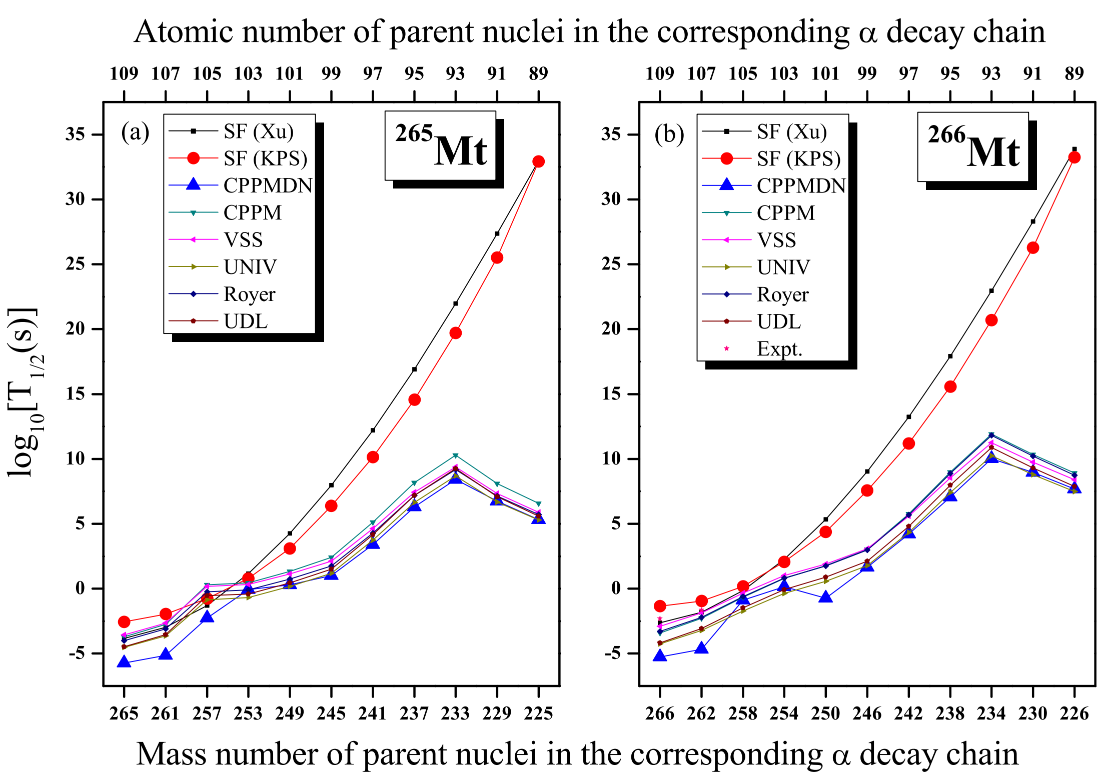

FIG. 1. The comparison of the calculated α-decay half-lives with the spontaneous fission half-lives for the isotopes ^{265,266}Mt and their decay products.

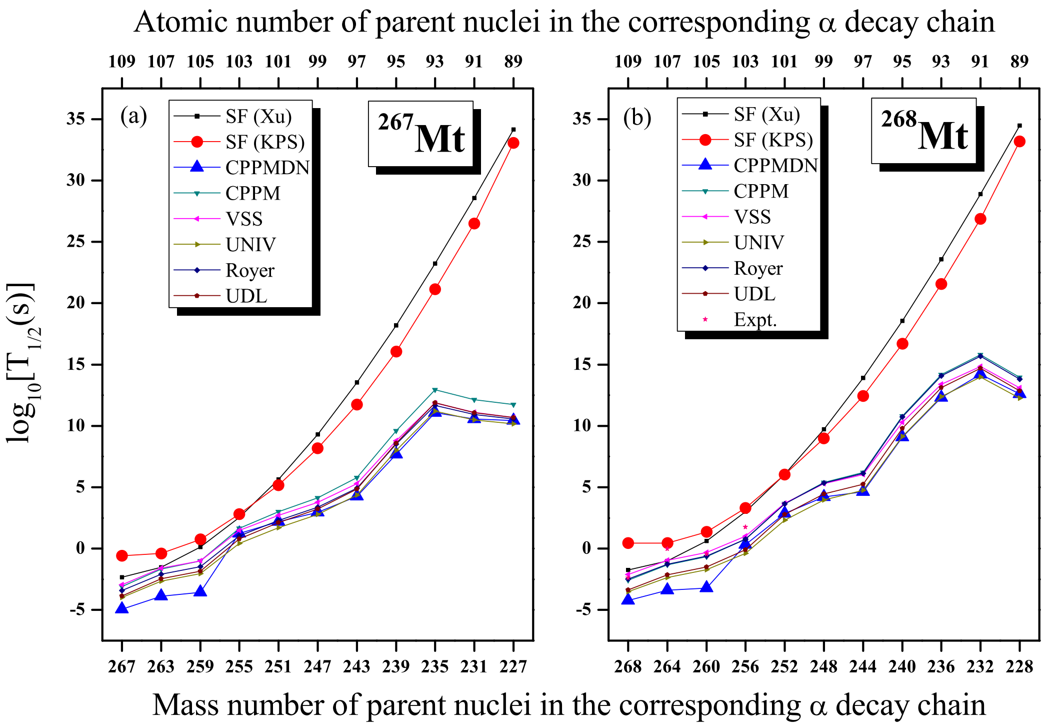

FIG. 2. The comparison of the calculated α-decay half-lives with the spontaneous fission half-lives for the isotopes ^{267,268}Mt and their decay products.

can be seen with different Q values. Experimental half-lives [30–33] of the isotopes, corresponding to the experimental decay modes are given in column 11. The theoretical and experimental predictions on the modes of decay are given in columns 12 and 13. The decay modes of the isotopes are predicted by comparing the α-decay half-lives calculated with the CPPMDN with the SF half-lives using the shell-effect-dependent formula of Santhosh and Nithya [34]. For isotopes

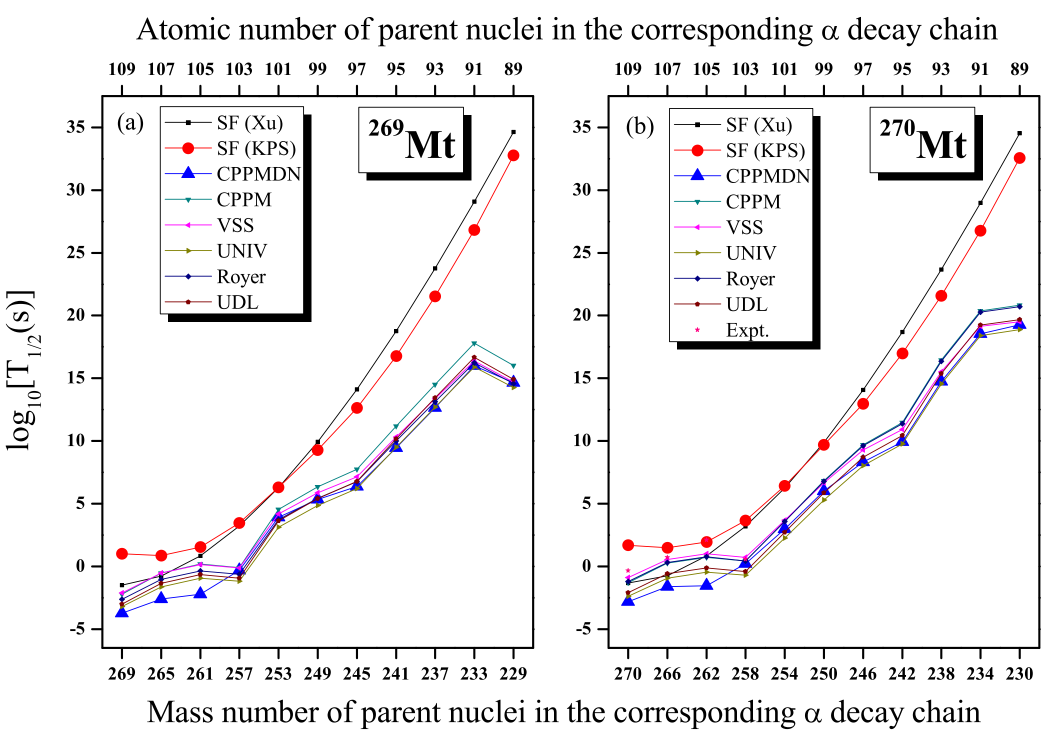

FIG. 3. The comparison of the calculated α-decay half-lives with the spontaneous fission half-lives for the isotopes ^{269,270}Mt and their decay products.

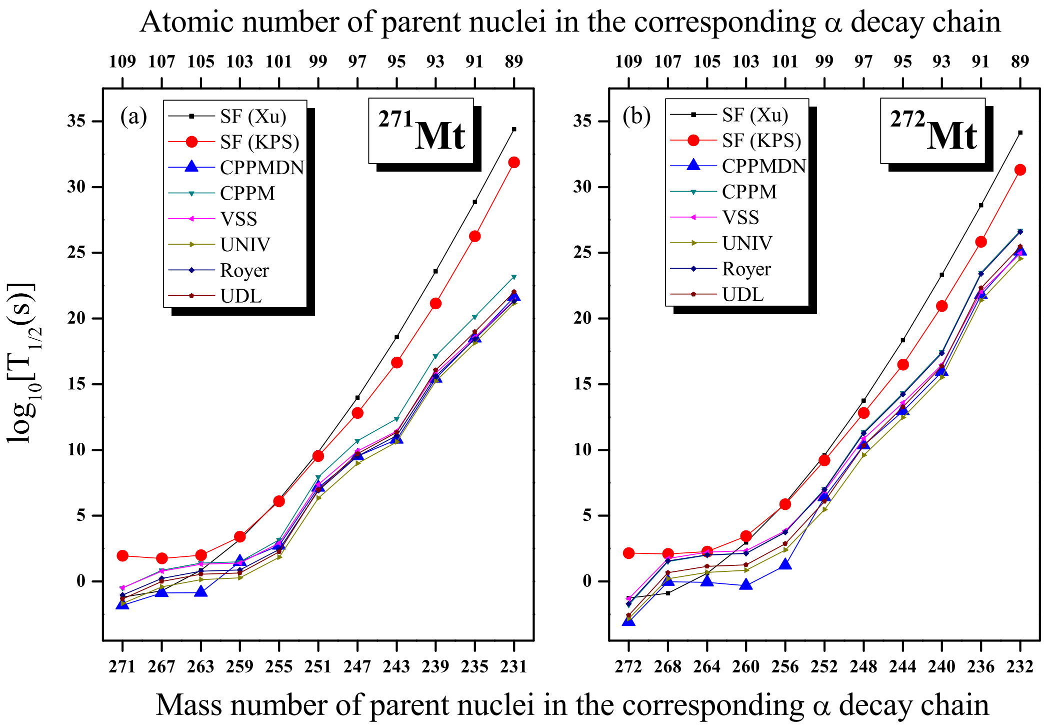

FIG. 4. The comparison of the calculated α-decay half-lives with the spontaneous fission half-lives for the isotopes ^{271,272}Mt and their decay products.

with $T_{1/2}^{\alpha} < T_{\mathrm{SF}}$, the α-decay dominates over SF. It is seen that the predictions on the decay modes match very well with the experimental results [30–33] for the isotopes $^{268,274-277}$Mt. For a better matching with the experimentally observed decay chain, in the case of ^{278}Mt, the α half-lives calculated using the CPPMDN are compared with the spontaneous fission half-lives of Smolańczuk *et al.* [24]. For ^{266}Mt, experimentally it was observed that after the second α chain, the isotope

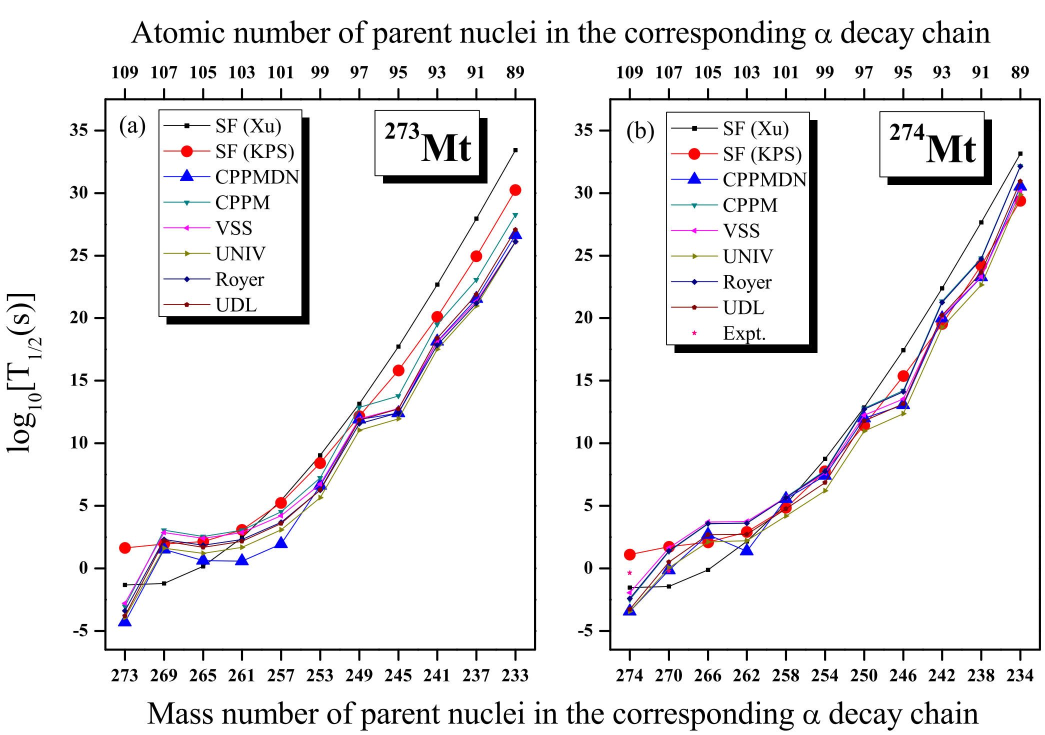

FIG. 5. The comparison of the calculated α-decay half-lives with the spontaneous fission half-lives for the isotopes ^{273,274}Mt and their decay products.

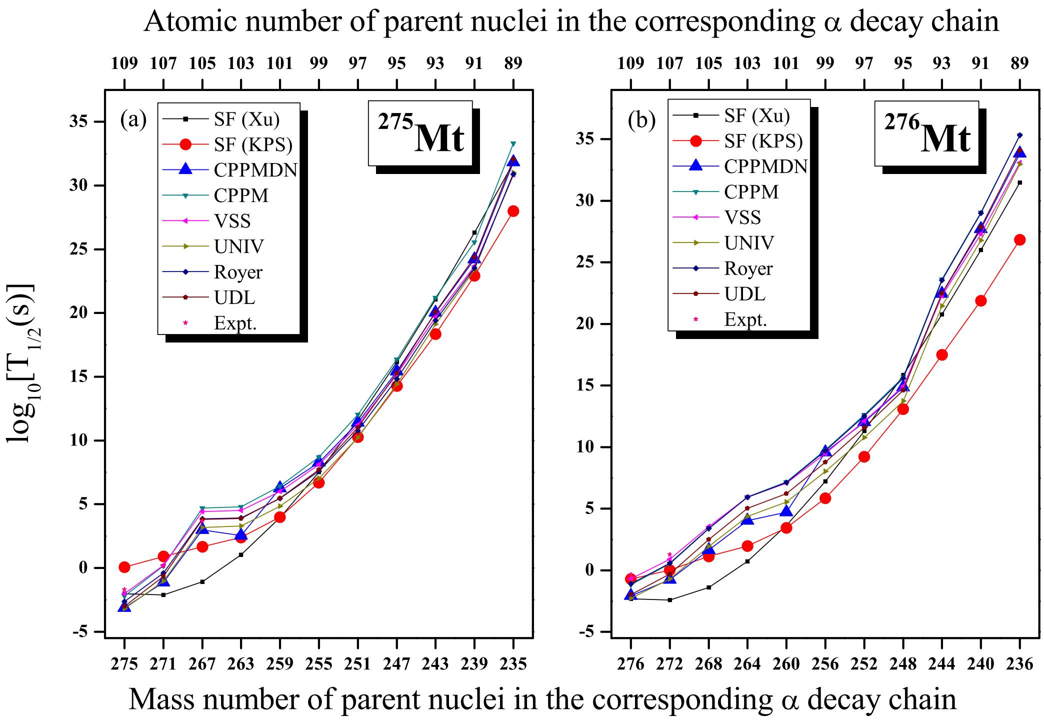

FIG. 6. The comparison of the calculated α-decay half-lives with the spontaneous fission half-lives for the isotopes ^{275,276}Mt and their decay products.

^{258}Db exhibits electron capture (EC) to form ^{258}Rf, which then decays by SF [30]. But theoretically long α chains are predicted from ^{266}Mt. Experimental results [69] show that the probabilities of electron capture for ^{258}Db are 35% and those of the α decay are 65%. After the fourth α chain, the decay product of the isotope ^{270}Mt, that is, ^{254}Md, also shows electron capture ($b_\varepsilon = 92\%$), and thereafter the daughter isotope ^{255}Fm will undergo α decay [32].

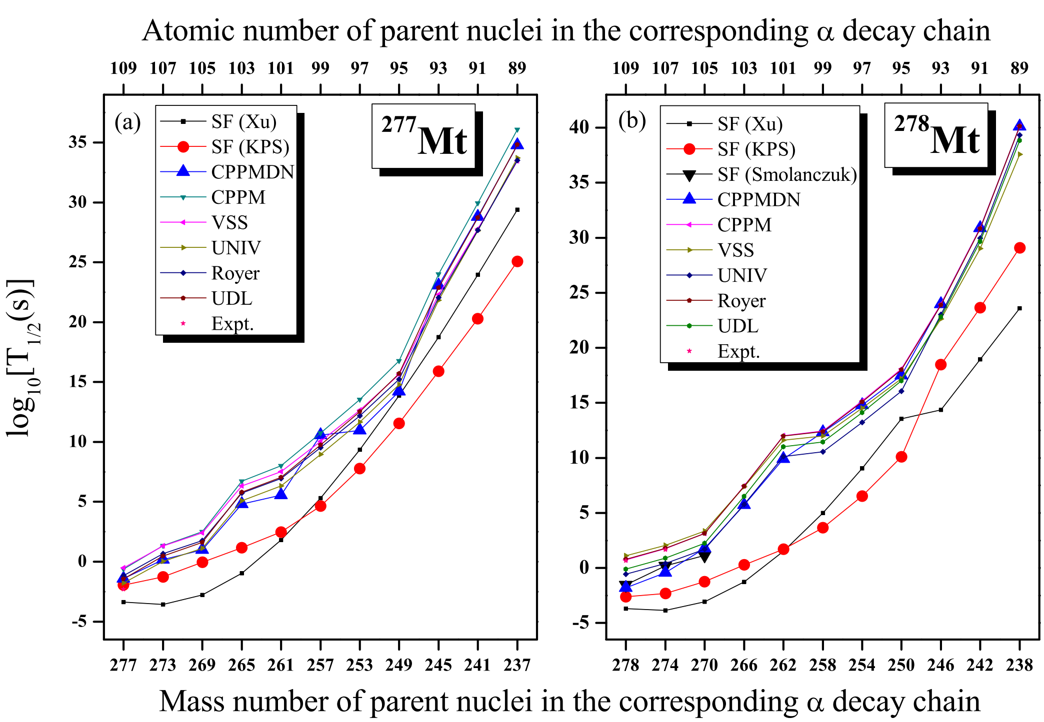

FIG. 7. The comparison of the calculated α-decay half-lives with the spontaneous fission half-lives for the isotopes ^{277,278}Mt and their decay products.

Since we are successful in reproducing the experimental decay modes of the isotopes $^{268,274\text{–}278}$Mt, we have confidently extended our study to predict the decay modes of all the isotopes of Mt within the range of $265 \leqslant A \leqslant 279$. The plots for the $\log_{10} T_{1/2}$ versus mass number of the parent nuclei for the isotopes $^{265\text{–}278}$Mt are shown in Figs. 1–7. From the figures, by comparing the α half-lives calculated using the CPPMDN (solid blue up triangle) with the SF half-lives by the shell-effect-dependent formula (solid red circle), it is seen that the isotopes $^{265,267,269,271\text{–}273}$Mt exhibit long α chains with half-lives within the experimental limits (for example, using the CPPMDN, $T^{\alpha}_{1/2} = 1.916 \times 10^{-6}$ s for ^{265}Mt; $T^{\alpha}_{1/2} = 1.175 \times 10^{-5}$ s for ^{267}Mt; $T^{\alpha}_{1/2} = 1.809 \times 10^{-4}$ s for ^{269}Mt; $T^{\alpha}_{1/2} = 1.569 \times 10^{-2}$ s for ^{271}Mt; $T^{\alpha}_{1/2} = 8.436 \times 10^{-4}$ s for ^{272}Mt, and $T^{\alpha}_{1/2} = 4.811 \times 10^{-5}$ s for ^{273}Mt). The isotope ^{279}Mt decays by SF since its SF half-life is less than the α half-life. As the predicted half-lives of the isotopes are within the experimental limit, we hope that our present paper, which predicts the modes of the decays of the isotopes $^{256\text{–}279}$Mt, will be very helpful in future experimental studies.

IV. CONCLUSIONS

Predictions on the α-decay chains of $^{265\text{–}279}$Mt are presented in the paper. The α-decay chains are predicted by comparing the α-decay half-lives within the CPPMDN of Santhosh *et al.* [25] with the spontaneous fission half-lives using the shell-effect-dependent formula of Santhosh and Nithya [34]. The predicted half-lives and decay modes match very well with the experimental results. The half-lives also are calculated with other theoretical formalisms for a comparison. Among four different mass tables used for calculating the α-decay energies, it is seen that the mass table of Wang *et al.* [56] is in better agreement with the experimental results for the isotopes in the decay chains of Mt. Long α chains are predicted from $^{265,267\text{–}269,271\text{–}273}$Mt with half-lives within the experimental limits. The isotopes $^{274\text{–}276,278}$Mt exhibit 2α chains followed by spontaneous fission. The 2α chain of ^{266}Mt and the 4α chain of ^{270}Mt end with electron capture. The isotopes ^{277,279}Mt decay via spontaneous fission. We hope that our paper will be useful for future experimental investigations in this field.

[1] U. Mosel and W. Greiner, Z. Phys. **222**, 261 (1969).
[2] S. G. Nilsson, C. F. Tsang, A. Sobiczewski, Z. Szymański, S. Wycech, C. Gustafson, I.-L. Lamm, P. Möller, and B. Nilsson, Nucl. Phys. A **131**, 1 (1969).
[3] W. D. Myers and W. J. Swiatecki, Ark. Fys. **36**, 343 (1967).
[4] H. Meldner, Ark. Fys. **36**, 593 (1967).
[5] A. Sobiczewski, F. A. Gareev, and B. N. Kalinkin, Phys. Lett. **22**, 500 (1966).
[6] S. Hofmann and G. Münzenberg, Rev. Mod. Phys. **72**, 733 (2000).
[7] Yu. Ts. Oganessian, J. Phys. G: Nucl. Part. Phys. **34**, R165 (2007).
[8] S. Hofmann, F. P. Heßberger, D. Ackermann, S. Antalic, P. Cagarda, B. Kindler, P. Kuusiniemi, M. Leino, B. Lommel, O. N. Malyshev, R. Mann, G. Münzenberg, A. G. Popeko, S. S'aro, B. Streicher, and A. V. Yeremin, Nucl. Phys. A **734**, 93 (2004).
[9] D. Ackermann, Nucl. Phys. A **787**, 353 (2007).
[10] K. Morita, Nucl. Phys. A **944**, 30 (2015).
[11] Yu. Ts. Oganessian and S. N. Dmitriev, Russ. Chem. Rev. **78**, 1077 (2009).
[12] D. N. Poenaru, M Ivaşcu, and A. Săndulescu, J. Phys. G: Nucl. Part. Phys. **5**, L169 (1979).
[13] B. Buck, A. C. Merchant, and S. M. Perez, Phys. Rev. C **45**, 2247 (1992).
[14] H. F. Zhang and G. Royer, Phys. Rev. C **76**, 047304 (2007).
[15] C. Qi, F. R. Xu, R. J. Liotta, and R. Wyss, Phys. Rev. Lett. **103**, 072501 (2009).
[16] C. Qi, F. R. Xu, R. J. Liotta, R. Wyss, M. Y. Zhang, C. Asawatangtrakuldee, and D. Hu, Phys. Rev. C **80**, 044326 (2009).
[17] B. A. Brown, Phys. Rev. C **46**, 811 (1992).
[18] V. E. Viola, Jr. and G. T. Seaborg, J. Inorg. Nucl. Chem. **28**, 741 (1966).
[19] W. J. Swiatecki, Phys. Rev. **100**, 937 (1955).
[20] D. W. Dorn, Phys. Rev. **121**, 1740 (1961).
[21] C. Xu and Z. Ren, Phys. Rev. C **71**, 014309 (2005).
[22] A. Staszczak, A. Baran, and W. Nazarewicz, Phys. Rev. C **87**, 024320 (2013).
[23] M. Warda and J. L. Egido, Phys. Rev. C **86**, 014322 (2012).
[24] R. Smolánczuk, J. Skalski, and A. Sobiczewski, Phys. Rev. C **52**, 1871 (1995).
[25] K. P. Santhosh, S. Sabina, and G. J. Jayesh, Nucl. Phys. A **850**, 34 (2011).
[26] K. P. Santhosh and C. Nithya, At. Data Nucl. Data Tables (2017). https://doi.org/10.1016/j.adt.2017.03.003
[27] K. P. Santhosh and C. Nithya, Eur. Phys. J. A **52**, 371 (2016).
[28] K. P. Santhosh, A. Augustine, C. Nithya, and B. Priyanka, Nucl. Phys. A **951**, 116 (2016).
[29] K. P. Santhosh and C. Nithya, Phys. Rev. C **95**, 054621 (2017).
[30] G. Münzenberg, W. Reisdorf, S. Hofmann, Y. K. Agarwal, F. P. Heßberger, K. Poppensieker, J. R. H. Schneider, W. F. W. Schneider, K.-H. Schmidt, H.-J. Schött, P. Armbruster, C.-C. Sahm, and D. Vermeulen, Z. Phys. A: At. Nucl. **315**, 145 (1984).
[31] S. Hofmann, F. P. Heßberger, D. Ackermann, G. Münzenberg, S. Antalic, P. Cagarda, B. Kindler, J. Kojouharova, M. Leino, B. Lommel, R. Mann, A. G. Popeko, S. Reshitko, S. Śaro, J. Uusitalo, and A. V. Yeremin, Eur. Phys. J. A **14**, 147 (2002).
[32] K. Morita, K. Morimoto, D. Kaji, H. Haba, K. Ozeki, Y. Kudou, T. Sumita, Y. Wakabayashi, A. Yoneda, K. Tanaka, S. Yamaki, R. Sakai, T. Akiyama, S.-i. Goto, H. Hasebe, M. Huang, T. Huang, E. Ideguchi, Y. Kasamatsu, K. Katori, Y. Kariya, H. Kikunaga, H. Koura, H. Kudo, A. Mashiko, K. Mayama, S.-i. Mitsuoka, T. Moriya, M. Murakami, H. Murayama, S. Namai, A. Ozawa, N. Sato, K. Sueki, M. Takeyama, F. Tokanai, T. Yamaguchi, and A. Yoshida, J. Phys. Soc. Jpn. **81**, 103201 (2012).
[33] Yu. Ts. Oganessian and V. K. Utyonkov, Rep. Prog. Phys. **78**, 036301 (2015).
[34] K. P. Santhosh and C. Nithya, Phys. Rev. C **94**, 054621 (2016).
[35] D. N. Poenaru, M. Ivaşcu, A. Săndulescu, and W. Greiner, Phys. Rev. C **32**, 572 (1985).

[36] C. Y. Wong, Phys. Rev. Lett. **31**, 766 (1973).
[37] N. Malhotra and R. K. Gupta, Phys. Rev. C **31**, 1179 (1985).
[38] R. K. Gupta, M. Balasubramaniam, R. Kumar, N. Singh, M. Manhas, and W. Greiner, J. Phys. G: Nucl. Part. Phys. **31**, 631 (2005).
[39] A. J. Baltz and B. F. Bayman, Phys. Rev. C **26**, 1969 (1982).
[40] Y. J. Shi and W. J. Swiatecki, Nucl. Phys. A **464**, 205 (1987).
[41] J. Blocki, J. Randrup, W. J. Swiatecki, and C. F. Tsang, Ann. Phys. (N.Y.) **105**, 427 (1977).
[42] J. Blocki and W. J. Swiatecki, Ann. Phys. (N.Y.) **132**, 53 (1981).
[43] N. Bohr and J. A. Wheeler, Phys. Rev. **56**, 426 (1939).
[44] K. P. Santhosh, R. K. Biju, and S. Sabina, Nucl. Phys. A **832**, 220 (2010).
[45] P. Möller, A. J. Sierk, T. Ichikawa, and H. Sagawa, At. Data Nucl. Data Tables **109–110**, 1 (2016).
[46] K. P. Santhosh and A. Joseph, Pramana **62**, 957 (2004).
[47] A. Sobiczewski, Z. Patyk, and S. Ćwiok, Phys. Lett. B **224**, 1 (1989).
[48] D. N. Poenaru, R. A. Gherghescu, and W. Greiner, Phys. Rev. C **83**, 014601 (2011).
[49] D. N. Poenaru, R. A. Gherghescu, and W. Greiner, Phys. Rev. C **85**, 034615 (2012).
[50] G. Royer, J. Phys. G: Nucl. Part. Phys. **26**, 1149 (2000).
[51] C. Xu, Z. Ren, and Y. Guo, Phys. Rev. C **78**, 044329 (2008).
[52] V. Yu. Denisov, O. I. Davidovskaya, and I. Yu. Sedykh, Phys. Rev. C **92**, 014602 (2015).
[53] G. Royer, Nucl. Phys. A **848**, 279 (2010).
[54] S. Zhang, Y. Zhang, J. Cui, and Y. Wang, Phys. Rev. C **95**, 014311 (2017).
[55] B. Sahu, R. Paira, and B. Rath, Nucl. Phys. A **908**, 40 (2013).
[56] M. Wang, G. Audi, F. G. Kondev, W. J. Huang, S. Naimi, and X. Xu, Chin. Phys. C **41**, 030003 (2017).
[57] V. Yu. Denisov and A. A. Khudenko, Phys. Rev. C **79**, 054614 (2009).
[58] K. N. Huang, M. Aoyagi, M. H. Chen, B. Crasemann, and H. Mark, At. Data Nucl. Data Tables **18**, 243 (1976).
[59] N. Wang, M. Liu, X. Z. Wu, and J. Meng, Phys. Lett. B **734**, 215 (2014).
[60] H. Koura, T. Tachibana, M. Uno, and M. Yamada, Prog. Theor. Phys. **113**, 305 (2005).
[61] X. J. Bao, S. Q. Guo, H. F. Zhang, and Q. Li, Phys. Rev. C **95**, 034323 (2017).
[62] M. Wang, G. Audi, A. H. Wapstra, F. G. Kondev, M. MacCormick, X. Xu, and B. Pfeiffer, Chin. Phys. C **36**, 1603 (2012).
[63] A. N. Kuzmina, G. G. Adamian, N. V. Antonenko, and W. Scheid, Phys. Rev. C **85**, 014319 (2012).
[64] A. Sobiczewski, Phys. Rev. C **94**, 051302(R) (2016).
[65] N. Wang and M. Liu, Phys. Rev. C **84**, 051303(R) (2011).
[66] A. Sobiczewski, J. Phys. G: Nucl. Part. Phys. **43**, 095106 (2016).
[67] Yu. A. Litvinov, M. Palczewski, E. A. Cherepanov, and A. Sobiczewski, Acta Phys. Pol., B **45**, 1979 (2014).
[68] Y. Z. Wang, S. J. Wang, Z. Y. Hou, and J. Z. Gu, Phys. Rev. C **92**, 064301 (2015).
[69] National Nuclear Data Center, Brookhaven National Laboratory, https://www.nndc.bnl.gov.